2007 IEEE International Conference on
Robotics and Automation
Roma, Italy, 10-14 April 2007

Design and Calibration of an Optical Micro Motion Sensing System for Micromanipulation Tasks

T. L. Win, U. X. Tan, C. Y. Shee and W. T. Ang, *Member, IEEE*

***Abstract*- An optical sensing system has been developed using a pair of orthogonally placed position sensitive detectors (PSD) to track 3D displacement of a microsurgical instrument tip in real-time. An infrared (IR) diode is used to illuminate the workspace. A ball is attached to the tip of an intraocular shaft to reflect IR rays onto the PSDs. Instrument tip position is then calculated from the centroid positions of reflected IR light on the respective PSDs. The system can be used to assess the accuracy of hand-held microsurgical instruments and operator performance in micromanipulation tasks, such as microsurgeries. In order to eliminate inherent nonlinearity of the PSDs and lenses, calibration is performed using a feedforward neural network. After calibration, percentage RMS error is reduced from about 5.46 % to about 0.16%. The system RMS noise is about 0.7 µm. The sampling rate of the system is 250 Hz.**

Keywords – **Position Sensitive Detectors, resolution, lenses, microsurgery, neural network**

I. Introduction

Vitreoretinal microsurgery and some cell micromanipulation tasks are fields that require very high tool positioning accuracy. In vitreoretinal microsurgery, there appears to be a consensus for the accuracy requirement of 10 µm [1] whilst cell micromanipulation tasks require accuracy ranging from micrometers to nanometers depending on the applications.

Many involuntary and inadvertent components are present in normal human hand movement. These include physiological tremor [2], jerk [3]and low frequency drift [4]. It has been reported that the vector magnitude of physiological tremor during the most delicate part of the procedure is measured to be 38 µm RMS [5].

Intelligent hand-held instruments have been or are being developed [6] to cancel tremor during microsurgery. We are also developing a similar instrument in our laboratory. In order to evaluate accuracy of such systems, more accurate systems need to be developed.

There are many commercial systems commonly used in tracking surgical instruments, including Optotrak (Northern Digital, Waterloo, Canada), Isotrack II (Polhemus, Colchester, Vt.) and miniBIRD. But, these systems cannot provide adequate accuracy and resolution for microsurgery and some cell micromanipulation applications.

To address the above issues, Riviere, C.N et al. developed ASAP (Apparatus to Sense Accuracy of Position) and MADRID (Measurement Apparatus to Distinguish Rotational and Irrotational Displacement) [7-9] systems to track microsurgical instrument motion in micro-scale. PSDs and lenses formed the main components of these systems whereby the accuracy is limited by nonlinearity inherent in PSDs and lenses.

It is well known that lens introduces distortion. PSD also introduces distortion effects that vary from PSD to PSD (Figure 1) and these distortion effects play a significant part at submicron and nanometer levels. The overall nonlinearity is the combination of distortion effects from the lenses and PSDs.

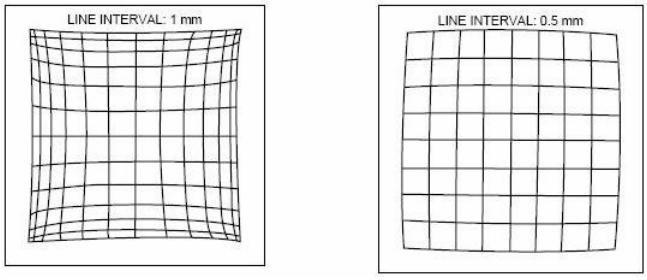

Figure 1. Distortion effect of PSDs

Accuracy is worse without calibration because of the imperfect alignment and assembly of the components. If accuracy and resolution can be improved by eliminating inherent nonlinearity and increasing signal to noise ratio respectively, the optical Micro Motion Sensing System (M2S2) can be extended to evaluate the accuracy of cell micromanipulation systems. This motivates us to develop a better tracking system and calibration method to eliminate nonlinearity.

Tun Latt Win is with the school of Mechanical and Aerospace Engineering, Nanyang Technological University, Singapore (phone: 65-9021-1975; fax: 65- 6793 5921; e-mail: wintunlatt@ntu.edu.sg).

U-Xuan Tan is with the school of Mechanical and Aerospace Engineering, Nanyang Technological University, Singapore (e-mail: TANU0002@ntu.edu.sg).

Cheng Yap Shee is with the school of Mechanical and Aerospace Engineering, Nanyang Technological University, Singapore (e-mail: cyshee@ntu.edu.sg)

Wei Tech Ang is with the school of Mechanical and Aerospace Engineering, Nanyang Technological University, Singapore (e-mail: wtang@ntu.edu.sg).

II. METHODOLOGY

A. System Development

We propose to use PSDs, instead of expensive high resolution and speed cameras as PSDs offer adequate high accuracy and frequency response at a lower and affordable cost. While CCD camera's resolution is limited by the number of pixels, that of PSD is limited by the noise floor of the system. There are four output electrodes for a two-dimensional PSD - two for each axis. The current produced at an electrode depends on the intensity and position of the light spot on the PSD. With regards to an electrode pair, the electrode located nearer to the light spot centroid will produce more current than the other. With this phenomenon, the position of the light spot centroid can be calculated once the current produced is known. Our system consists of two PSDs, three lenses, one IR diode, a white reflective ball and a data acquisition (DAQ) system as shown in Figure 2. and Figure 3. The overall system block diagram is shown in Figure 4.

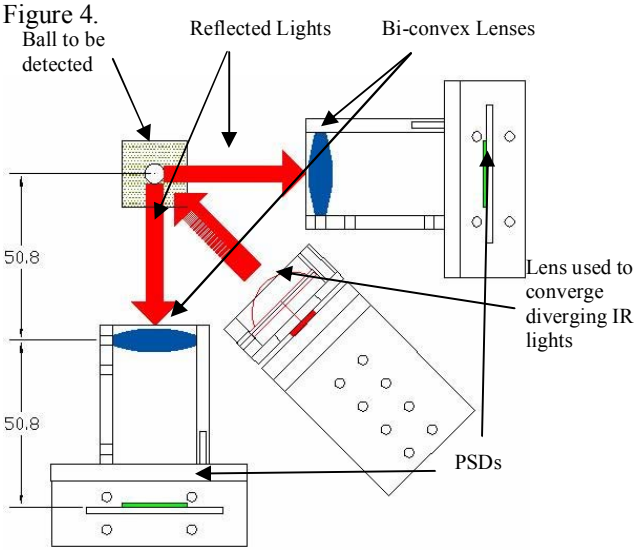

Figure 2. Schematic Diagram (Top View) of the system

A white reflective ball (Diameter=6mm) from Gutermann (Art. 773891), which is to be tracked, is attached to a non-reflective black color rod of 1 mm in diameter. IR light is shined onto the workspace containing the ball so that IR light reflected by the ball would impinge on the PSDs. The light spot positions on the respective PSDs are affected by the ball position.

Two PSD modules (DL100-7PCBA3) each with a 10mm square sensing area from Pacific Silicon Sensor Inc are used in our system and placed orthogonally to each other (Figure 2. and Figure 3.). There are four bipolar analog voltages outputs from each PSD module - X position (X_{diff}) and Y position (Y_{diff}) of the light spot centroid as well as the total X current (X_{sum}) and Y current (Y_{sum}). The schematic diagram of a PSD module is shown in Figure 5. The sum outputs (X_{sum}, Y_{sum}) are used to normalize the difference outputs (X_{diff} and Y_{diff}) so that the X and Y positions become independent of fluctuations in light spot intensity. The position calculation is shown in the equations below.

Normalized X position = $(X1-X2)/(X1+X2) = X_{diff}/X_{sum}$
Normalized Y position = $(Y1-Y2)/(Y1+Y2) = Y_{diff}/Y_{sum}$

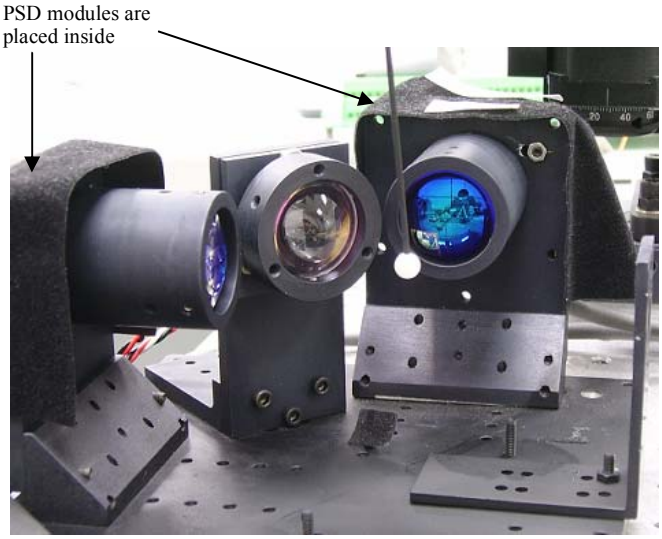

Figure 3. Micro Motion Sensing System (MMSS)

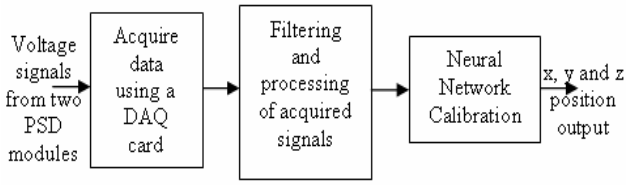

Figure 4. Overall block diagram of the system (MMSS)

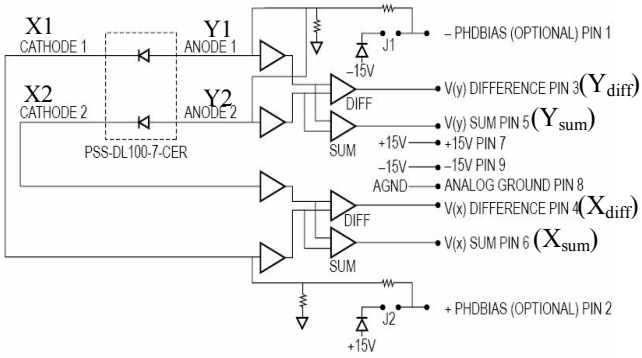

Figure 5. Schematic Diagram of a DL100-7PCBA3 PSD module.

Voltage signals from each output of the PSD modules are sampled and digitized at 16 bits, 16.67 kHz using the PD2-MF-150 data acquisition card from United Electronic Industries, Inc. Shielded cables are used to connect every PSD module output to the data acquisition card for better noise suppression. The power and signal cables are also separated to eliminate coupling of power line noise and signals. The digitized samples are first filtered with an 8th

order Butterworth low-pass software filter having a cutoff frequency of 15Hz and subsequently averaged every 67 samples. Thus, the sampling rate is 16.67k/67=248Hz. The unfiltered and filtered signal noise is about 10mV and less than 0.5mV respectively. After averaging, the filtered signals are used to compute the respective normalized position values - x1, z1, y2 and z2. Finally, the normalized values are applied to the input of a feedforward neural network to obtain the absolute position x, y and z.

Bi-convex lenses (Diameter=25.4mm, f=25.4mm) from Thorlabs (LB1761-B) are used to focus the reflected IR light onto the PSDs. These anti-reflection lenses also reduce surface reflection to maximize the IR light intensity striking the PSDs. Without the bi-convex lenses, the reflected IR light would impinge on the PSDs in such a manner that the position of the ball position cannot be determined correctly.

The system resolution is determined by the signal to noise ratio (SNR). Higher system SNR would offer better resolution. The intensity and wavelength of reflected IR light striking the PSDs are important factors in increasing SNR. The intensity must be high enough whilst the IR light wavelength must fall within the most sensitive region of the PSD spectral response. We choose OD-669 IR diode from Opto Diode Corp. as the IR light source because it has the highest power output and its peak emission wavelength is within the most sensitive region of the PSD spectral response. Since radiation of IR light from OD-669 is diverging, an aspheric condenser lens (D=27mm, EFL=13mm) from Edmund Optics is placed in front of the IR diode to converge the IR rays onto the workspace. The lens also enhances the IR intensity by more than 2 times. The IR diode is strobed at 500Hz (Duty cycle=50%) thereby increasing the maximum current limit of the IR diode. This results in a higher IR emission intensity and thereby, improving the SNR. The strobe timing of the IR diode is controlled with a PIC microcontroller via a field effect transistor (FET).

B. System Calibration

Calibration of the system can be performed by various approaches such as physical modeling, brute force method in which look-up table (LUT) and interpolation are used, neural network, etc. Physical modeling can give the best accuracy if done accurately and that requires thorough understanding of the physical behavior of each individual component. LUT with interpolation method requires calibration data points be stored in memory and needs more data points for higher accuracy.

We propose to employ a multilayer neural network approach for this application because it eliminates the need to know individual component's behavior; uses a reasonable span of time for a trained network to determine the output and can approximate any arbitrary continuous function to any desired degree of accuracy [10].

The calibration data points are obtained by moving the ball being tracked to known locations and using the corresponding values from the two PSDs. Movement of the ball is automatically done by controlling motorized precision stages using software developed in-house. X-Y-Z stepper-motorized precision translation stages (8MT173-20 from Standa) are used for our calibration. According to the specifications, 1 step movement of the stepper motors is equivalent to 1.8 degrees rotational and 1.25 micrometer translational movement respectively. The step angle accuracy is 5%. Since our data points spacing is 500 micrometers which is an integer multiple of 1.25 micrometers, the accuracy is 1.25*0.05= 62 nanometers. The travel range is 20mm. The calibration setup for the system is shown in Figure 6.

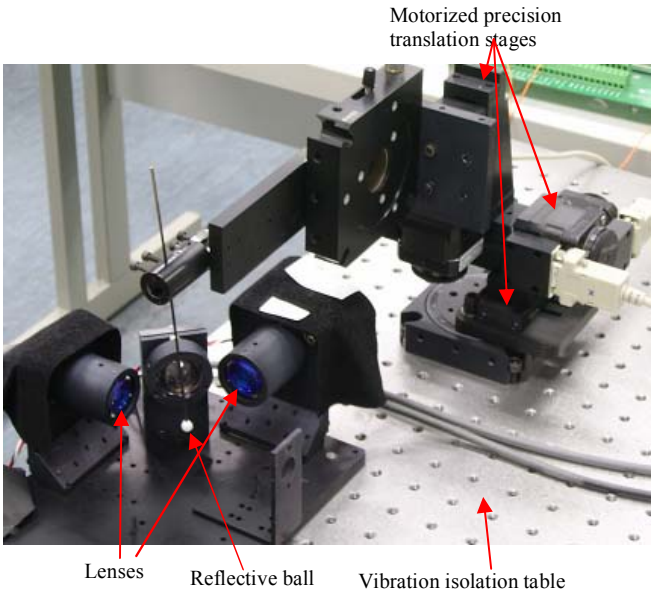

Figure 6. MMSS system and its calibration setup

The exact region of workspace is not initially known due to imperfect alignment and assembly of the PSDs and lenses. A 20mm cubical region is initially scanned with a step increment of 1mm between two successive points to cover the workspace region. The 20mm cubical region is large enough for estimating the workspace region based on our knowledge of the system configuration and sensing area of the PSDs.

Matlab is then used to plot these initial calibration data points in a 3 dimensional graph to determine the workspace region.

We then trained the neural network using calibration data points spaced 0.5mm apart for the range of 6.5mm in each axis. Therefore, total number of calibration points used is 13x13x13=2197. The training data is limited within a 6.5 mm cubical region to attain accurate neural network output since the degree of nonlinearity outside the said region is too high. This high degree of nonlinearity is assumed to be due to the imperfect alignment and distortion effects of lenses and PSDs. As such, the useful working region is limited to 6.5mm cubical region although 10mm square sensing area

PSDs is used. The normalized positions obtained at each calibration point and their corresponding absolute positions are used as training and target values respectively for neural network training. The network was also trained in a similar manner using calibration points with 1 mm spacing.

In order to improve the quality of the acquired data, after every step movement, sufficient time is provided for mechanical vibrations generated by the motion of the motorized stages to settle down before acquiring data. In addition, the system including the motorized stages is placed on an anti-vibration table to suppress floor emanated vibrations.

In order to ensure that calibration is not affected by temperature, the system is switched on for about 50 minutes before commencing calibration so that the IR diode attained a steady operating temperature state.

C. *Software Implementation and Integration*

LabVIEW, a signal acquisition, measurement and analysis software from National Instrument Corporation, is used to acquire, filter, and process signals from the PSDs. Neural network function is implemented in C language and integrated within the LabVIEW based program developed.

Since acquisition takes place continuously while the IR diode is strobing, the acquired signals contained voltage values whilst the IR diode was switched on (ON-time) and off (OFF-time). However, only voltage values acquired during ON-time contained relevant position information of the ball being tracked. Therefore, acquired voltage values are separated and only ON-time values used for subsequent processing. The segregation of ON-time and OFF-time voltage values is carried out using a software threshold approach described hereafter.

In this approach, a transistor-transistor logic (TTL) signal having the same switching frequency and phase as the signal controlling the IR diode is used as the reference signal. TTL is about 5V and 0V during ON-time and OFF-time respectively. A data acquisition channel is used to acquire the TTL signal and subsequently, compared with a predefined threshold value of 4V.

One scan is defined as a period during which sampling takes place channel after channel for all active data acquisition channels. In a scan, if the acquired TTL value is above the threshold, all voltage values acquired during that scan are regarded as ON-time values and used for processing. On the other hand, if the TTL value is below the threshold, all acquired voltage values are considered as OFF-time values and not used for processing.

There is a fixed amount of time-delay between sampling of each successive channel. So, there is a possibility that some channels' values are OFF-time values while the TTL signal indicates ON-time. To make sure that only ON-time values are used in processing, the first scan of any IR diode switching cycle in which the TTL signal indicates ON-time is not used.

D. *Mapping by a Feedforward Neural Network*

We propose a multilayer artificial neural network model because PSD calibration is a nonlinear problem that cannot be solved using a single layer network [11]. The determination of proper network architecture for the PSD system calibration is ambiguous like other neural network applications. The best architecture and algorithm for a particular problem can only be evaluated by experimentation and there are no fixed rules to determine the ideal network model for a problem. However, variations in architecture and algorithm affect only the convergence time of the solution.

The network model we employed includes 4 input neurons, and 3 output neurons. The number of neurons in the hidden layers and the number of layers are varied to achieve the best accuracy. Four neurons are used in the input layer because there are four inputs; x1, y1, y2 and z2. Three neurons are used in the output layer for the three coordinates; x, y and z. Transfer functions of all the layers are log-sigmoid except for the output layer, which is a linear function. The block diagram of the model is shown in Figure 7.

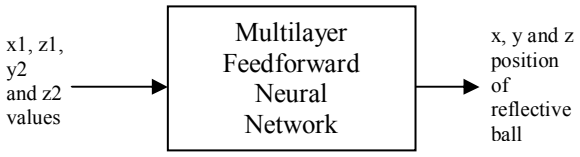

Figure 7. Nonlinear mapping provided by a multilayer feedforward neural network

III. RESULTS

The improvement in linearity after the calibration using a neural network is shown in figure 8(b) and 9(b). The amount of improvement is shown in Table I. All results presented in the tables are obtained from the neural network trained using points with 0.5mm spacing. The neural network consists of 4, 20, and 20 neurons in the first, second, and third hidden layers respectively and 3 neurons in the output layer. The results obtained using training points having 1mm spacing are not as good as those shown in the tables.

Percentage errors (RMSE (%) and Maximum Error (%)) are calculated over the range of 6.5mm cubical region. To determine the measurement errors at each point, measured values at these locations are subtracted from their respective true values. True values are known by moving the ball to be tracked to known locations using the motorized stages. Then, average RMS error and maximum error values are calculated using errors at all the points. The RMS errors calculated within different sizes of cubical regions are shown in Table II.

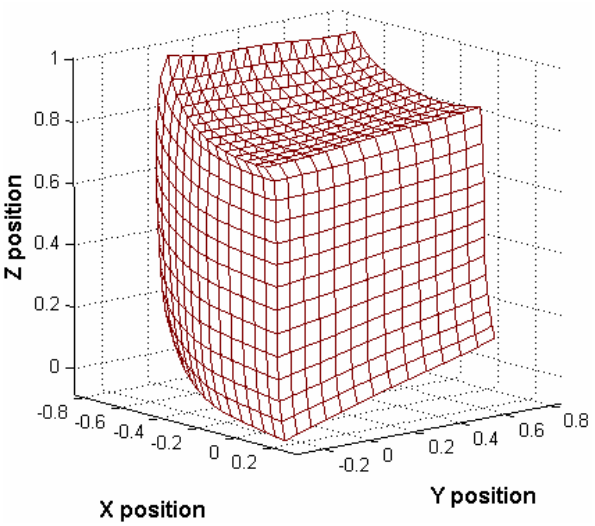

(a)

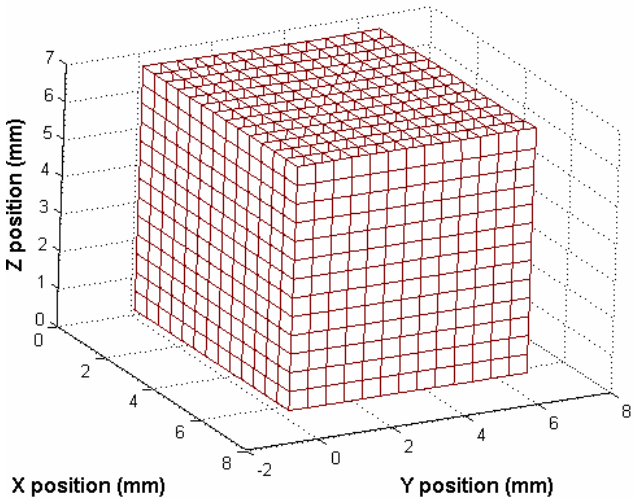

(b)

Figure 8. 3D Comparison for the amount of non-linearity (a) before calibration, and (b) after neural network calibration.

In order to determine resolution of the system, a one minute recording of a stationary ball position is obtained. The RMS noise is found to be 0.7μm.

The resolution of the system with a larger ball (diameter 10mm) is also tested. The RMS noise for a one minute position recording is discovered to be 0.5μm.

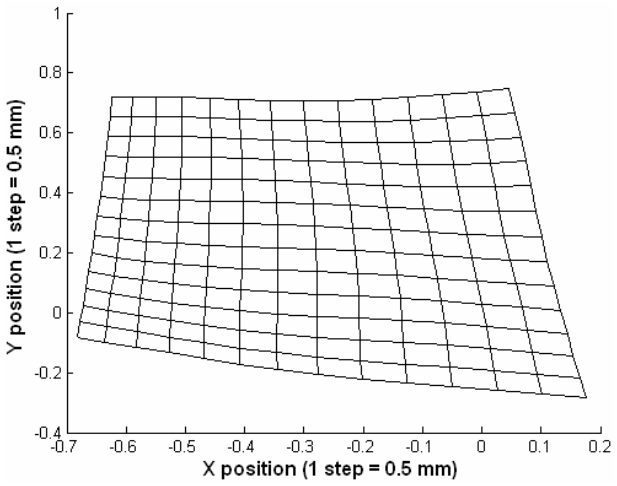

(a)

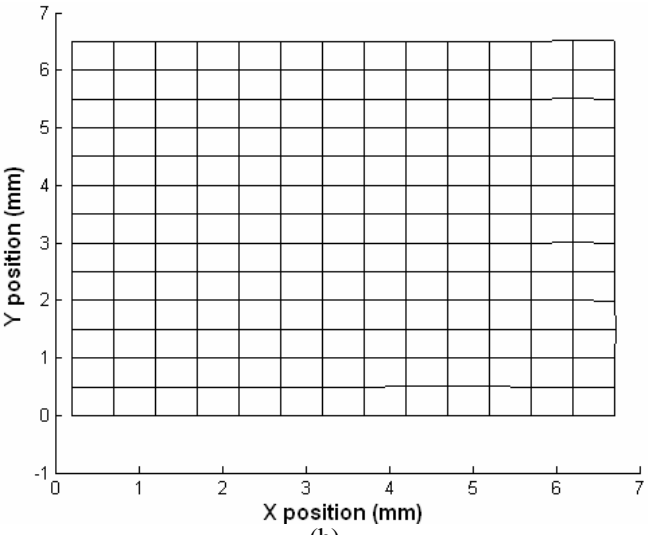

(b)

Figure 9. 2D Comparison for the amount of non-linearity (a) before calibration, and (b) after neural network calibration.

TABLE I. ERROR DUE TO NONLINEARITY BEFORE CALIBRATION AND AFTER CALIBRATION $\frac{RMSE}{6500}$ (%)

	Before Calibration	After Calibration
RMSE (μm)	354.89	10.22
$\frac{RMSE}{6500}$ (%)	5.46	0.16
Maximum Error (μm)	1483.10	74.40
$\frac{MaxError}{6500}$ (%)	22.82	1.14

TABLE II. RMS ERROR CALCULATED WITHIN DIFFERENT SIZES OF CUBICAL REGION

Cubical Region (mm^3)	RMSE (μm)
1.5	3.49
2.5	3.99
3.5	4.70
4.5	5.40
5.5	6.39
6.5	10.22

IV. DISCUSSION

The RMSE values stated in Table II show that errors increase with larger working region. This suggests that nonlinearity is less severe near to the center of the workspace and manipulation tasks should be performed near to the centre for better tracking accuracy.

RMS noise is lesser with a bigger ball as more reflected IR rays are produced thereby increasing the intensity of the IR light striking the PSDs. Although a smaller ball size is preferred for microsurgical trainings, some applications that require better resolution and where the ball size is not a major concern, can use a larger diameter ball.

Since the system employs optical approach, line-of-sight between PSDs and the ball has to be maintained. This hampers the use of this system for tracking in actual microsurgical operations. However, for accuracy evaluation of microsurgical instruments or performance of surgeons, the setup can be arranged such that the IR light path between PSDs and the ball will not be blocked.

Comparing to other similar systems [7-8], our system offers better performance in terms of sampling rate and resolution. The sampling rate of our system is 250 Hz while other similar systems are 150 Hz. The resolution of our system is 0.7μm while other systems are in the region of 1μm. Comparison of accuracy against other systems cannot be made because other systems do not describe overall system accuracy.

V. CONCLUSION

We have developed a real-time optical micro-motion sensing system that utilized a multi-layer feedforward neural network approach for its nonlinear calibration. The results suggested that nonlinearity is eliminated thereby greatly improving the linearity. More subsequent experiments involving varying architectures and calibration data is expected to yield better results. The future work includes improving resolution by providing additional light sources and utilizing better IR reflective material for the ball (such as gold).

VI. ACKNOWLEDGMENT

Intelligent Handheld Instrument for Microsurgery & Biotech Micromanipulation project is funded by Agency for Science, Technology & Research (A*STAR) and the College of Engineering, Nanyang Technological University. The authors thank them for the financial support of this work.

REFERENCES

[1] S. Charles, "Dexterity enhancement for surgery," *Computer Integrated Surgery: Technology and Clinical Applications*, MA: MIT Press, pp. 467–472, 1996.

[2] R. C. Harwell, and Ferguson. R. L, "Physiologic tremor and microsurgery," *Microsurgery*, vol. 4, pp. 187-192, 1983.

[3] P. S. Schenker, et al. "Development of a telemanipulator for dexterity enhanced microsurgery," *Proc. 2nd Int. Symp. Med. Rob. Comput. Assist. Surg.*, 1995.

[4] L. Hotraphinyo, and C. N. Riviere, "Three-dimensional accuracy assessment of eye surgeons," *Proc. 23rd Annu. Conf. IEEE Eng. Med. Biol. Soc.*, Istanbul, 2001.

[5] S. P. N. Singh, and C. N. Riviere, "Physiological Tremor Amplitude during Retinal Microsurgery," *Proc. 28th Annu. International Conference of the IEEE Northeast Bioengineering Conference*, pp. 171-172, Apr. 2002.

[6] C. N. Riviere, W. T. Ang, and P. K. Khosla, "Toward Active Tremor Canceling in Handheld Microsurgical Instruments," *IEEE Transactions on Robotics and Automation*, vol. 19, No. 5, pp. 793-800, Oct. 2003.

[7] L. F. Hotraphinyo, and C. N. Riviere. "Precision Measurement for Microsurgical Instrument Evaluation," *Proc. of the 23rd Annu. EMBS International Conference,* Istanbul, Turkey, 2001.

[8] C. N. Riviere, and P. K. Khosla, "Microscale Tracking of Surgical Instrument Motion," *Proc. 2nd Intl. Conf. on Medical Image Computing and Computer-Assisted Intervention,* Cambridge, England, 1999.

[9] R. Ortiz, and C. N. Riviere, "Tracking Rotation and Translation of Laser Microsurgical Instrument," *Proc. of the 25th Annu. International Conference of the IEEE EMBS*, Caneum, Mexico, 2003.

[10] K. Funahashi, "On the approximation realization of continuous mapping by neural networks," *Neural Networks*, vol. 2, pp. 183-192, 1989.

[11] L. V. Fausett, "*Fundamentals of Neural Networks: Architectures, Algorithms and Applications,"* Prentice-Hall, 1994, pp. 289-330.